AJNR

High-flow angiopathy: cerebral blood vessel changes in experimental chronic arteriovenous fistula.

J M Pile-Spellman, K F Baker, T M Liszczak, B B Sandrew, R F Oot, G Debrun, N T Zervas and J M Taveras

AJNR Am J Neuroradiol 1986, 7 (5) 811-815
http://www.ajnr.org/content/7/5/811

High-Flow Angiopathy:
Cerebral Blood Vessel Changes in Experimental Chronic Arteriovenous Fistula

John M. D. Pile-Spellman[1]
Keith F. Baker[2]
Theodore M. Liszczak[2]
Barry B. Sandrew[1]
Robert F. Oot[1]
Gerard Debrun[1,3]
Nicholas T. Zervas[2]
Juan M. Taveras[1]

Profound vascular damage secondary to high-flow extracranial states has been well characterized. However, changes in cerebral vasculature secondary to high-flow states have not been studied. To determine changes related to high-flow states in cerebral vessels, a rabbit model was developed in which torrential flow was created in the vertebrals, carotids, basilar, and vessels of the circle of Willis by means of a carotid-jugular shunt after ligation of the proximal carotid. The clinical, angiographic, and histologic changes noted in the animal model include: (1) abrupt clinical deterioration after a variable interval with some animals developing ptosis, (2) afferent vessel dilatation and the development of prominent anastomotic channels, (3) variable cerebral vessel histopathology—related to duration and relative proximity to the shunt—affecting all three vessel layers, (4) plump, irregular, and clumped endothelium, denuded with adherent platelets, (5) irregular, duplicated, and thinned internal elastic membrane, frayed with invasion of the intima by mesenchymal cells, (6) vacuolization and necrosis of the media muscle, and (7) invasion of adventitia by foreign cells and small blood vessels. The high-flow angiopathy seen in this model may help explain vascular changes associated with high-flow cerebral vascular lesions, as well as other types of vascular damage.

High flow rates and velocities [1–3] that have been associated with vascular damage to extracranial vessels are also known to occur in cerebral arteriovenous malformations (AVMs) and fistulas [4, 5]. Histologic changes in surgically resected AVMs show extensive and profound vascular disease; however, it is not clear if these changes are secondary to the deleterious effects of high flow per se or are part of the primary disease. These changes include an increase in the size, length, and number of the vessels; intimal thickening and destruction; elastic degeneration; irregular thickening or thinning of vessel walls with thrombosis, recannalization, and siderosis; and an increase in the number of very small vessels [6]. The angiographic evidence of vascular changes include ectasia and tortuosity [7], aneurysm formation [8], stenosis, and thrombosis of arterial feeders and venous drainage [9, 10]. This study documents the clinical, pathologic, and angiographic changes associated with high-flow cerebral vascular states in an experimental model.

Materials and Methods

New Zealand rabbits (n = 16) were anesthetized and maintained with halothane (1–2%). After intubation, the left carotid artery and the external jugular were aseptically disected and the proximal common carotid artery was ligated. The distal common carotid stump was then joined to the external jugular vein with an end-to-end anastomosis using microsurgical technique (Fig. 1). The distal external carotid was ligated in the initial animals to simplify surgery. The incision was sutured and the animal allowed to recover.

Clinical inspection of the animals was performed to note focal neurologic signs. Animals showing signs of systemic illness or weakness had angiography and were then sacrificed by

Received February 13, 1986; accepted after revision May 9, 1986.

Presented at the annual meeting of the American Society of Neuroradiology, San Diego, January 1986.

This work was supported in part by a grant from the Edward M. Mallinckrodt Foundation awarded to J. M. D. Pile-Spellman; by an XARCHIVE Neuroscience Research Grant awarded to the Neuroscience Imaging Laboratory in the Department of Radiology; and by NIH grant HL-22573-08 awarded to N. T. Zervas.

[1] Department of Radiology, Massachusetts General Hospital and Harvard Medical School, Boston, MA 02114. Address reprint requests to J. M. D. Pile-Spellman.

[2] Department of Neurosurgery, Massachusetts General Hospital and Harvard Medical School, Boston, MA 02114.

[3] Present address: Department of Radiology, Johns Hopkins University, Baltimore, MD 21205.

AJNR 7:811–815, September/October 1986
0195–6108/86/0705–0811

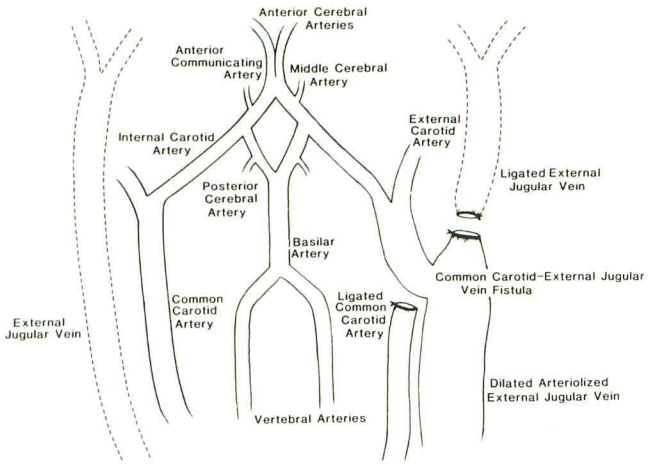

Fig. 1.—Anatomic diagram showing cephalic vessels and carotid jugular fistula.

gluteraldehyde perfusion under halothane anesthesia. All remaining animals were sacrificed in a similar fashion after 9 months, regardless of their clinical condition. Autopsy was performed on any animal with an acute demise; however, histologic examination was performed only on animals that were sacrificed acutely and adequately perfused.

Angiograms were performed by either the retrograde axillary or transfemoral route via a cutdown. A mid-arterial film was obtained during hand injection of 3–4 ml of Conray 60 (Mallinckrodt; iothalamate meglumine) into the aortic arch with an anode-film distance of 40 in. and an anode-animal distance of 38 in. The angiograms were used to assess and grade: (1) ectasia, (2) anastomotic prominence, (3) shunt patency and prominence, and (4) the size of the cerebral vessels. A measure of the vascular dilatation was obtained by adding the measured diameter of the mid-basilar, plus a vertebral at the C1 level and a carotid artery. When both carotids or vertebrals were well visualized, a mean of the two was used in the calculation. Because of the difficulty in routinely identifying the postcommunal portion of the posterior communication artery, for our purposes the term "posterior communicating artery" includes the precommunal portion of the posterior cerebral artery.

At sacrifice, the animals were perfused with saline followed by gluteraldehyde (2.5%); the brains were inspected grossly after removal. The cerebral vessels after post fixation in 2% Dalton's chrome osmium were embedded in epoxy resin and thin-sectioned. They were examined by both light and transmission microscopy for vascular disease.

Controls consisted of 20 normal New Zealand rabbits in which angiography and histology were performed in identical ways.

Results

A total of 16 rabbits underwent distal carotid-jugular anastomosis and proximal carotid ligation.

Survival and Morbidity

The mean survival time was 5.85 weeks (SEM ± 2.8), with a range of 0.5–35.9. A majority of the animals (12 of 16) underwent an abrupt deterioration characterized by lethargy after an initial healthy period, with sudden death occurring in four animals. Autopsy failed to reveal cardiopulmonary cause of death in any animal. Intermittent unilateral ptosis on the side of the shunt, or ataxia, was seen in three animals. Inspection of the brain revealed blood surrounding the basilar artery, suggesting subarachnoid hemorrhage in three animals.

Angiographic Changes

Half the animals were sufficiently stable to survive angiography (Figs. 2 and 3). The time of angiography ranged from 0.86 to 35.9 weeks after surgery, with a mean of 16.4 weeks. The afferent vessels leading to the shunt—including the vertebrals, carotids, basilar, and circle of Willis—were moderately to markedly tortuous in all animals (seven of eight) that had angiograms at 6 or more weeks post surgery. While these changes were not prominent in the single animal who underwent angiography 6 days after surgery, they were seen in the single animal with thrombosis of the fistula on angiography. The additive measure of vascular dilation as described above was 5.78 mm (SEM ± 1.9) vs 3.11 mm (SEM ± 0.15) for normals. Of all the vessels, the internal carotid artery and posterior communicating artery ipsilateral to the shunt consistently showed the greatest dilation. Anastomotic channels—including costocervical to vertebral, occipital to vertebral, maxillary to ethmoidal, and external carotid to external carotid—were present in a majority of animals (five of eight). These channels were seen in only those animals that had marked flow through the shunt at the time of angiography. Shunt patency and prominence were graded as torrential in four of eight animals, marked in one of eight, discernible in two of eight, and thrombosed in one of eight.

Histopathology

Thirty cerebral vessels from eight animals were examined histologically. They ranged from 1.2–35 weeks post surgery, with a mean of 15.0 (SEM ± 3.6). The vessels showing the greatest histologic changes were those closest to the shunt. In the same animal, the left posterior communicating artery showed more severe changes relative to the right posterior communicating artery. Nonafferent cerebral vessels—i.e., the middle cerebral artery—showed no evidence of disease (Fig. 4).

Progressive pathological changes were noted over time. The early events were characterized by changes in the endothelium. These changes, seen as early as 8 days after surgery, consisted of rounding and protrusion of the endothelial cells into the vascular lumen. This was followed by desquamation, platelet adherence, and attempts at reendothelialization (Figs. 5 and 6). This reendothelialization was characterized by migration of mononucleated cells onto and among the adherent platelets. Weibel-Palade bodies, cellular inclusions typically found in endothelial cells, were not seen in these cells. Smooth-muscle vacuolization occurred early after desquamation but was not seen in later stages. Typical mesenchymal cell proliferation was observed in response to

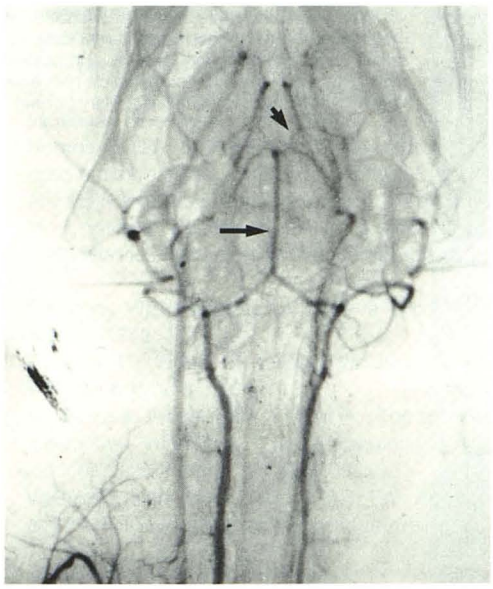

2

Fig. 2.—Anteroposterior view from a normal rabbit cerebral angiogram. Note normal size of basilar (*arrow*) and very small posterior communicating artery (*arrowhead*).

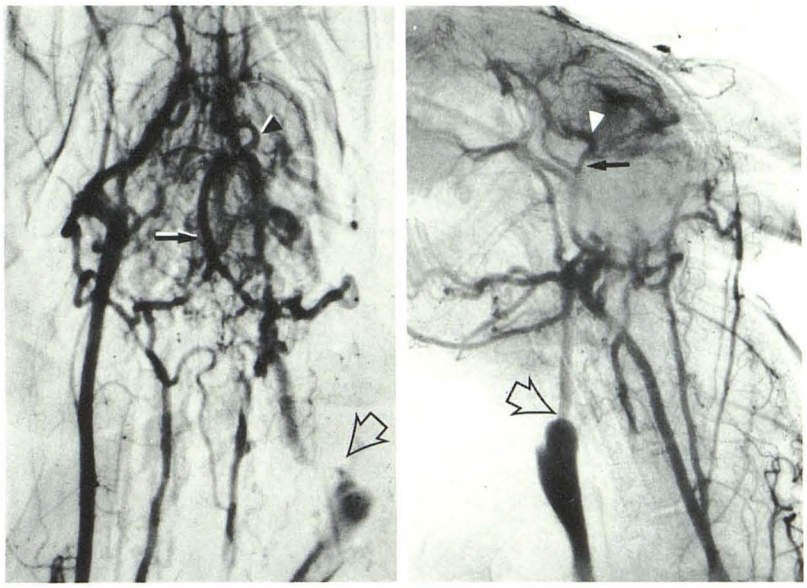

A B

Fig. 3.—Anteroposterior (**A**) and lateral (**B**) views of rabbit after proximal carotid artery ligation and distal carotid artery–external jugular anastomosis (*open arrow*). Note anastomosis, which, while patent, has undergone stenosis. The afferent vessels to fistula—including carotid arteries and vertebrals as well as basilar (*straight arrow*) and vessels of circle of Willis, particularly left posterior communicating artery *(arrowhead)*—are markedly dilated. Prominent extra- and intracranial anastomotic channels are seen.

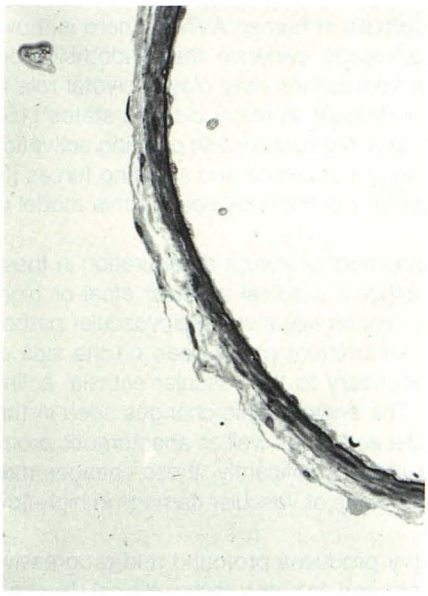

4

Fig. 4.—Normal right middle cerebral artery. Note flattened, almost indistinguishable endothelial cell, a thin dark continuous internal elastic lamina, uniform vacuole-free smooth muscle cells, and adventitia free of vessels and foreign cells. (Magnification = 950×)

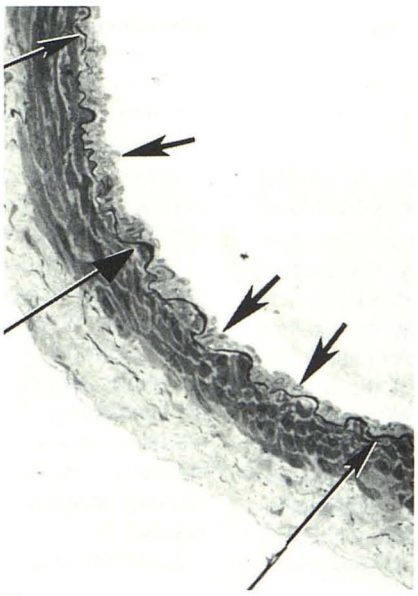

5

Fig. 5.—Posterior communicating artery showing corrugation of internal elastic lamina (*thin long arrows*), adherent platelets, and nucleated cell (*thick short arrows*). (Magnification = 950×)

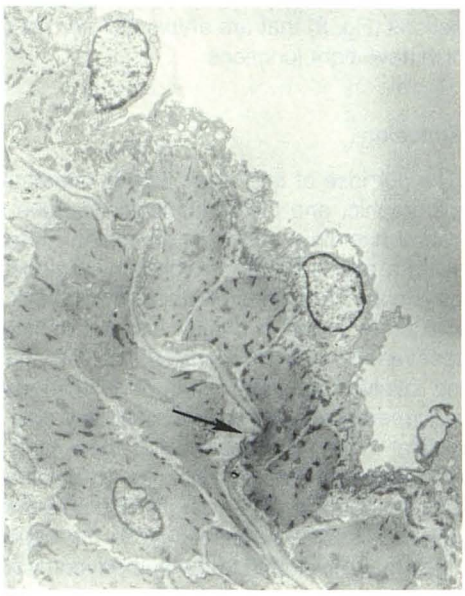

6

Fig. 6.—Electron micrograph showing migration of smooth muscle cells through breaks in internal elastic lamina (*arrow*). Note absence of endothelial cells with their characteristic cytoplasmic Weibel-Palade bodies. (Magnification = 6500×)

7

Fig. 7.—Basilar artery showing absence of internal elastic lamina. Abnormal adherent cells of luminal surface consists of platelets and nucleated cells. Note proliferating smooth muscle cells against luminal surface and adventitial capillary (*arrow*).

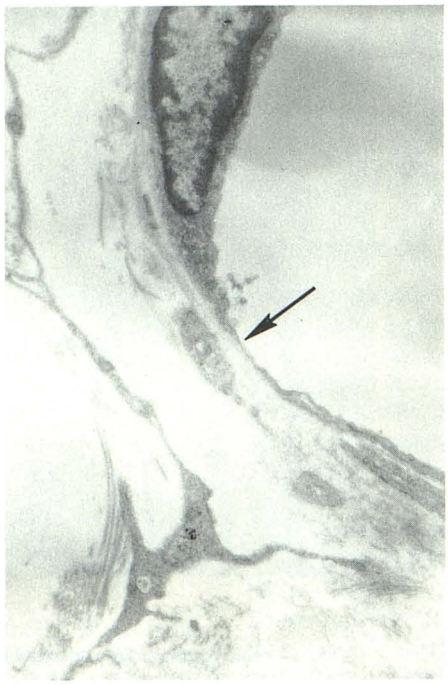

8

Fig. 8.—Ultrastructural demonstration of same capillary seen in Figure 7 with fenestrated endothelial junction (*arrow*). (Magnification = 17,000×)

desquamation. In addition, capillary proliferation was observed in the adventitia (Fig. 7). These new vessels in the adventitia, characterized as capillaries because of their lack of smooth muscle, possess fenestrated, "leaky," endothelial junctions (Fig. 8) that are atypical of normal cerebral arteries, which have tight junctions.

Discussion

The purpose of this study was to characterize the clinical, angiographic, and histopathologic changes associated with cerebral high-flow states in otherwise normal animals. Employing a rabbit model of high-flow angiopathy, the present study demonstrated histopathologic changes remarkably similar to those found in human surgical pathology in high-flow arteriovenous malformations [6, 11, 12]. In both cases, disease involves not only destructive changes of the internal elastic membrane and endothelium, but also alteration of the muscular layer. In human AVM specimens the plethora of small vessels without a muscular layer—that is, the associated telangectatic [6] or primitive embryologic components [13]—are similar in appearance to the capillaries within adventitia that developed in the hemodynamically stressed vessels of the present model. The development of these new capillaries without the characteristics of an intact blood-brain barrier is clearly abnormal [14]. The histopathology of high-flow angiopathy in our rabbit preparation raises doubts as to the primacy of these findings as the "nidus." Indeed, that these small vessels are also seen in the periphery of surgically resected AVMs suggests that they may in fact simply be anastomotic collaterals. Failure to consider the profound effects of hemodynamic stress on the angioarchitecture of normal vessels associated with an AVM may be confounding our current understanding of AVMs.

Because of early postmortem changes, less is known about the pathology of endothelia in human AVMs. There is, however, abundant experimental evidence that endothelial destruction and platelet interactions may play a pivotal role in the initiation of vessel damage in many disease states [15]. Endothelium damage and destruction with ongoing activation of platelets attributable to turbulence and shearing forces [3] may account for much of the changes seen in this model of high-flow angiopathy.

Clinically, the development of abrupt deterioration in these animals may reflect either a cerebral vascular steal or high-output cardiac failure despite negative cardiovascular pathology at autopsy. The intermittent ptosis seen on the side of the shunt may be secondary to the vascular ectasia, acting as a mass (Fig. 3B). The angiographic changes seen in this model of marked vessel ectasia as well as anastomotic prominence is well appreciated. Significantly, these changes may represent angiographic signs of vascular damage in high-flow states.

High-flow angiopathy produces profound and progressive angiographic, histologic, and, in some cases, clinical changes. This model may be useful not only in the study of these states but also in experimental interventional radiology.

REFERENCES

1. Stehbens WE. Blood vessel changes in chronic experimental arteriovenous fistula. *Surg Gynecol Obstet* **1968**;127:327–331
2. Davis PF, Stehbens WE. The biochemical composition of hae-

modynamically stressed vascular tissue. Part I: The lipid, calcium and DNA concentrations in experimental arteriovenous fistulae. *Atherosclerosis* **1985**;56:27–37
3. Fry DL. Acute vascular endothelial changes associated with increased blood velocities gradients. *Circ Res* **1968**;22:165–197
4. Nornes H, Grip A. Hemodynamic aspects of cerebral arteriovenous malformations. *J Neurosurg* **1980**;53:456–464
5. Ancri D, Pertuiset B. Instantaneous measurements of flow velocity in internal carotid arteries by pulsed Doppler in cerebral arteriovenous malformation. *Neurochirurgie* (*Stuttg*) **1985**;31:1–6
6. Stehbens WE. *Pathology of cerebral blood vessels*. St Louis: Mosby, **1972**
7. Taveras JT, Wood EH. *Diagnostic neuroradiology*. Baltimore: Williams & Wilkins, **1976**
8. Miyasaka K, Wolpert SM, Prager RJ. The association of cerebral aneurysms, infundibulum and intracranial arteriovenous malformations. *Stroke* **1982**;13:196–203
9. Vinuela F, Nombela L, Roach MR, Fox AJ, Pelz DM. Stenotic and occlusive disease of the venous drainage system of deep brain AVMs. *J Neurosurg* **1985**;63:180–184
10. Mawad ME, Hilal SK, Michelson WJ, Stien B, Ganti SR. Occlusive disease associated with cerebral arteriovenous malformations. *Radiology* **1984**;153:401–408
11. McCormick WF. The pathology of vascular ("arteriovenous") malformations. *J Neurosurg* **1966**;24:807
12. Paillas JE, Berard M, Sedan R, Toga M, Alliez B. The relative importance of atheroma in the clinical coarse of arteriovenous angioma of the brain. In: Luyendijk W, ed. *Cerebral circulation*, spec. iss. of *Prog Brain Res* **1968**;30:419
13. Isoda K, Fukuda H, Takamura N, Humamoto Y. Arteriovenous malformation of the brain—histological study and micrometric measurement of abnormal vessels. *Acta Pathol Jpn* **1981**;31:883–893
14. Liszczak TM, Black PMcL, Varsos VG, Zervas NT. Microcirculation of cerebral arteries: a morphological and morphometric examination of the major canine cerebral arteries. *Am J Anat* **1984**;170:223–232
15. Ross R, Glomset JA. The pathogenesis of atherosclerosis. *N Engl J Med* **1977**;295:369–377